USGS
science for a changing world

Prepared in cooperation with Marin County Flood Control District

Stratigraphic Analysis of Corte Madera Creek Flood Control Channel Deposits

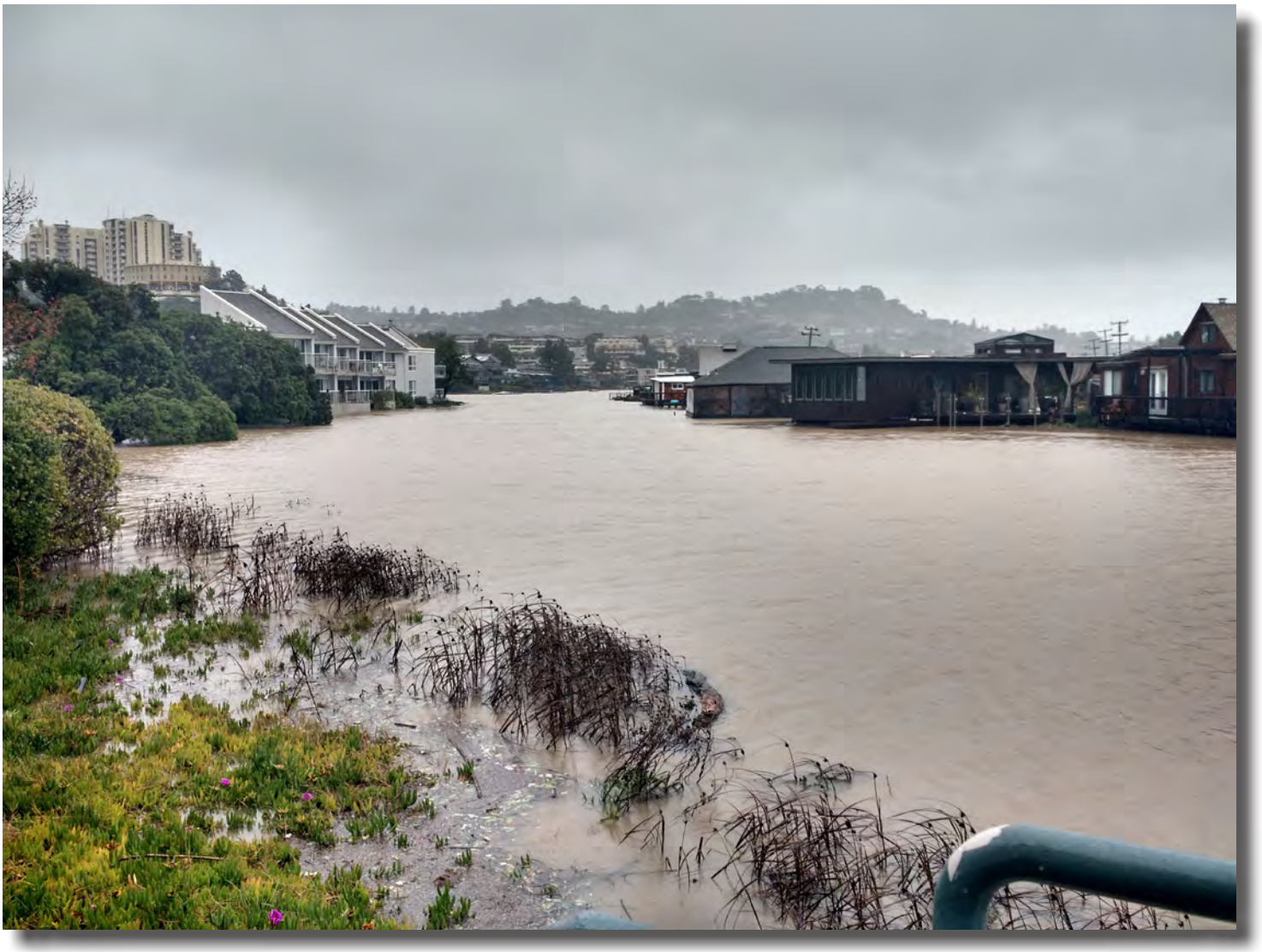

Scientific Investigations Report 2019–5070

U.S. Department of the Interior
U.S. Geological Survey

Cover photo: Corte Madera Creek flooding. Photograph taken by Deb Etheredge, January 10, 2017, licensed under CC BY 2.0

Stratigraphic Analysis of Corte Madera Creek Flood Control Channel Deposits

By Daniel Livsey, Paul Work, and Maureen Downing-Kunz

Prepared in cooperation with Marin County Flood Control District

Scientific Investigations Report 2019–5070

U.S. Department of the Interior
U.S. Geological Survey

U.S. Department of the Interior
DAVID BERNHARDT, Secretary

U.S. Geological Survey
James F. Reilly II, Director

U.S. Geological Survey, Reston, Virginia: 2019

Suggested citation:
Livsey, D., Work, P., and Downing-Kunz, M., 2019, Stratigraphic analysis of Corte Madera Creek flood control channel deposits: U.S. Geological Survey Scientific Investigation Report 2019–5070, 28 p., https://doi.org/10.3133/sir20195070.

ISSN 2328-0328 (online)

Acknowledgments

The authors would like to acknowledge financial support from the Marin County Flood Control District, helpful review comments from Stetson Engineers of San Rafael, California, and Scott Dusterhoff of the San Francisco Estuary Institute, Richmond, California.

The authors also would like to acknowledge assistance in the field from Daniel Powers and SeanPaul La Selle of the U.S. Geological Survey Pacific Coastal and Marine Geology office, Santa Cruz, California and timely and helpful reviews by Renee Takesue of the U.S. Geological Survey Pacific Coastal and Marine Science Center.

Contents

Figures

Tables

Conversion Factors

International System of Units to U.S. customary units

Multiply	By	To obtain
	Length	
centimeter (cm)	0.3937	inch (in.)
millimeter (mm)	0.03937	inch (in.)
meter (m)	3.281	foot (ft)
kilometer (km)	0.6214	mile (mi)
meter (m)	1.094	yard (yd)
	Area	
square meter (m^2)	0.0002471	acre
square kilometer (km^2)	247.1	acre
square centimeter (cm^2)	0.001076	square foot (ft^2)
square meter (m^2)	10.76	square foot (ft^2)
hectare (ha)	0.003861	square mile (mi^2)
square kilometer (km^2)	0.3861	square mile (mi2)
	Volume	
cubic meter (m^3)	35.31	cubic foot (ft^3)
cubic meter (m^3)	1.308	cubic yard (yd^3)
	Speed and Flow rate	
meter per second (m/s)	3.281	foot per second (ft/s)
cubic meter per second (m^3/s)	35.31	cubic foot per second (ft^3/s)
	Mass to Weight	
gram (g)	0.03527	ounce (oz)
kilogram (kg)	2.205	pound (lb)
metric ton (t)	1.102	ton, short [2,000 lb]
metric ton (t)	0.9842	ton, long [2,240 lb]
	Shear Stress	
Newton per square meter (N/m^2) or pascal (Pa)	0.0001450	pound-force per square inch (lbf/in^2)

Temperature in degrees Celsius (°C) may be converted to degrees Fahrenheit (°F) as $°F = (1.8 \times °C) + 32$.

Temperature in degrees Fahrenheit (°F) may be converted to degrees Celsius (°C) as $°C = (°F - 32) / 1.8$.

Datum

Vertical coordinate information is referenced to the North American Vertical Datum of 1988 (NAVD 88).

Horizontal coordinate information is referenced to the North American Datum of 1983 (NAD 83).

Elevation, as used in this report, refers to distance above the vertical datum.

Abbreviations

D_{50}	median grain size, by weight
D_{90}	grain size exceeded by only 10 percent of a sample, by weight
MHHW	mean higher high water
MLLW	mean lower low water
MTL	mean tide level
NWIS	National Water Information System
USACE	U.S. Army Corps of Engineers
USGS	U.S. Geological Survey
WY	water year (October 1–September 30)

Stratigraphic Analysis of Corte Madera Creek Flood Control Channel Deposits

By Daniel Livsey, Paul Work, and Maureen Downing-Kunz

Abstract

Sedimentation in a channel can reduce flood conveyance capability and potentially place nearby property and life at risk from flooding. In 1998, Marin County Public Works dredged the concrete-lined segment of Corte Madera Creek, which drains a hilly and largely urbanized watershed that terminates in San Francisco Bay, California. From then through 2015, approximately 4,100 cubic meters of sand and gravel infilled the concrete-lined segment. Determining when and under what conditions this material was deposited informs dredging operations for the Corte Madera Creek Flood Control Project and increases understanding of sediment delivery timing and mechanisms from this and other San Francisco Bay tributaries.

Two hypothesized scenarios were investigated: (1) complete flushing during high flows and re-deposition of channel fill afterward and (2) more steady, gradual channel infilling. Stratigraphic analysis of eight sediment cores collected from the flood-control channel deposits in August 2017 was used to identify the most likely scenario. In addition, sediment elevation profiles, grain-size data, and a one-dimensional hydrodynamic model were used to assess the potential for longitudinal-channel scour and deposition following the wet winter of water year 2017 in the intertidal reach of the concrete channel in Corte Madera Creek.

Results indicated the channel is undergoing gradual infilling. Storm flows of water year 2017 did not completely scour the concrete channel fill. Sediment cores, stratigraphic analysis, and sediment elevation profiles indicated 0.23 meter of scour at the downstream end of the concrete-lined section and that roughly 0.5 meter of channel fill remained in the channel. The hydrodynamic model demonstrated that sediment deposition in the concrete channel is expected to start downstream from the point where the channel bed reaches mean lower low-water level. High flows can carry most of the sediment through this segment of channel, depositing the bed-material load downstream from the transition to a wide channel, where velocity and bed shear stress decrease abruptly.

Although the storm flows of 2017 did not completely scour the channel fill, subsequent material deposited in the channel could be transported downstream from the concrete channel if the sediment elevation profile is in equilibrium with present (2019) mean sea level. A calibrated, coupled hydrodynamic-sediment transport model could be used to test the present equilibrium between sediment elevation profiles and mean sea level, such that additional sediment build-up in the concrete channel is remobilized during subsequent wet-season flows and deposited downstream from the concrete-lined segment.

Introduction

Corte Madera Creek in Marin County, California, delivers runoff from a hilly and largely urbanized watershed to the western side of the central part of San Francisco Bay (Stetson Engineers, 2000). The U.S. Geological Survey (USGS) maintains a streamflow gage on Corte Madera Creek, upstream from the reach that is the focus of this report (Station 11460000; data available at https://waterdata.usgs.gov/nwis/dv/?site_no=11460000). Discharge measurements at this station began in 1951.

The lower, tidally influenced reach of Corte Madera Creek was designed to convey flood waters as part of the Corte Madera Creek Flood Control Project (fig. 1). The reach of interest includes a concrete-lined channel with a deeper section that serves as a stilling basin at its downstream end, transitioning to a wider earthen channel that terminates in San Francisco Bay.

Sedimentation in a channel can reduce flood conveyance capability and potentially place nearby property and life at risk of flooding. In 1998, Marin County Public Works dredged the concrete-lined segment of the channel. Between 1998 and 2015, approximately 4,100 cubic meters (m^3) of sand and gravel infilled the concrete-lined part of the channel to a maximum observed thickness of approximately 1.4 meters (m) in the stilling basin (U.S. Army Corps of Engineers, 2016a). Determining how and when this material was deposited would inform dredging operations for the Corte Madera Creek Flood Control Project and increase understanding of sediment delivery timing and mechanisms from this and other San Francisco Bay tributaries.

The work described here was not intended to be a comprehensive investigation of the watershed or long-term processes (Stetson Engineers, 2000; Kamman, 2014).

Figure 1. Study area, concrete-lined channel segment, and sampled reach in lower Corte Madera Creek, Marin County, California.

This work was aimed specifically at testing two conceptual models describing recent (months to years) sediment deposition in the concrete channel section of Corte Madera Creek, upstream from San Francisco Bay. Specifically, the two scenarios investigated were (1) complete flushing during and re-deposition of channel fill after high-flow events and (2) more steady, gradual channel infilling (fig. 2). In the gradual infilling scenario, finer estuarine muds are interbedded with the coarser, terrestrially derived channel fill. Stratigraphic analysis from sediment cores collected from the flood control channel fill were used to ascertain if the channel fill either (1) is completely scoured and replaced during peak flows or (2) has aggraded episodically since the 1998 dredging. In addition, sediment elevation profiles, grain-size data, and a one-dimensional hydrodynamic model were utilized to investigate the potential for longitudinal-channel scour and deposition following the wet season of water year (WY) 2017 in the intertidal portion of the concrete channel section in Corte Madera Creek.

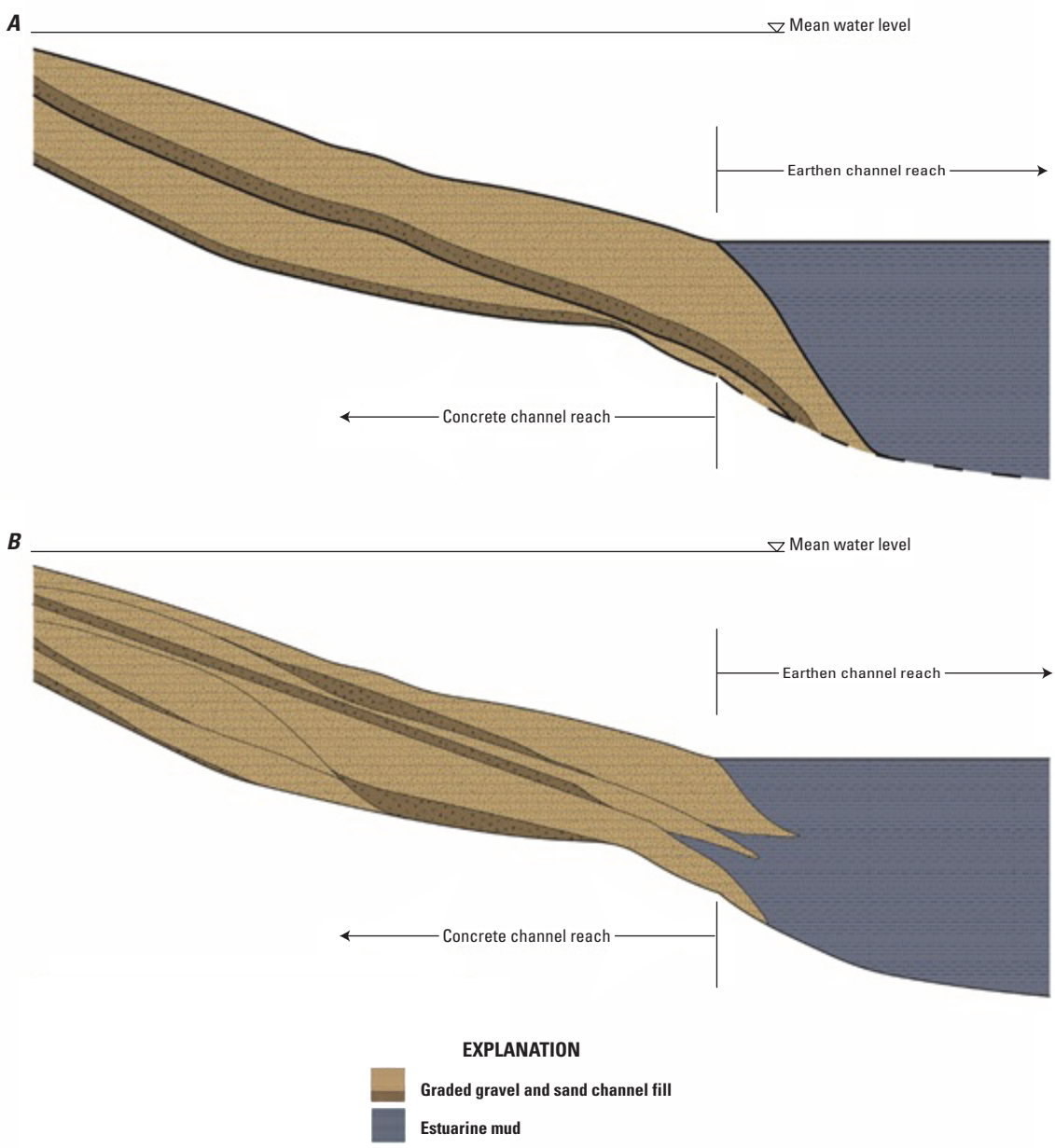

Figure 2. Alternative depositional models for channel fill in Corte Madera Creek flood control channel, Marin County, California. Longitudinal profile view of the channel shown. *A*, Channel fill is completely flushed annually and re-deposited during high flows in the wet season. *B*, Channel fill has aggraded episodically since last dredging operation in 1998, resulting in channel stratigraphy featuring nested, normally graded deposits interbedded with estuarine silts and clays at the concrete-lined channel terminus.

Field Methods

Eight 7.6 centimeter (cm) diameter cores were collected along a 0.43 kilometer (km) longitudinal transect from below the downstream end of concrete-lined channel, upstream to College Avenue (fig. 3) to investigate the channel fill stratigraphy. Cores were collected from a pontoon boat equipped with a winch in August, near the end of the normally dry season, of water year (WY) 2017. A 7.6-cm aluminum pipe was driven into the channel fill using a gasoline-powered concrete vibrator, and the winch was used to extract the core from the sediment. Core-surface elevations were determined from a May 2017 elevation survey by Stetson Engineers (2017). Longitudinal stations from previous elevation surveys are cited for comparison to previous work in the channel. Modern depositional environments and sedimentary characteristics were described during field reconnaissance on July 18, 2017, to allow interpretation of the sediment deposits in the cores. All grain-size classifications (for example, mud, sand, pebble) accord to the Wentworth grain-size scale (Wentworth, 1922) with additional textural classifications for pebbles of fine (2–8 millimeters, or mm), medium (8–16 mm), and coarse (16–64 mm), following Williams and others (2006).

Seven cores were collected from Corte Madera Creek on August 24, 2017 (table 1 and fig. 3). Farthest downstream, core CM17_01 sampled an intertidal bar just downstream (bayward) from the downstream end of the concrete section of the channel. Continuing upstream, cores CM17_02, CM17_03, and CM17_07 sampled the stilling basin approximately 15 m (50 ft) upstream from the downstream end of the concrete channel section. Cores CM17_05 and CM17_06 were collected at stations designated as 4 and 5, respectively, by Stetson Engineers (2017).

Initially, two fluked boat anchors were utilized to hold the vessel on station while sampling; this proved inadequate for obtaining the desired vertical cores. As a result, Cores CM17_01, CM17_02, and CM17_03 were driven with the coring tube at an angle (less than 30 degrees from vertical). To hold the vessel on station better, lines were used to secure the bow and stern of the sampling platform to shore. As a result of this improved method, cores CM17_04, CM17_05, CM17_06, and CM17_07 were driven in closer to vertical. Cores sampled at an angle overestimate actual sediment layer thicknesses; the associated depth errors (proportional to 1 divided by the cosine of the tilt angle) were accounted for when estimating sediment thicknesses in the cores (table 1). Cores CM17_01, CM17_02, and CM17_03 were assumed to be 30 degrees from vertical; a value of 15 degrees was assumed for cores CM17_04, CM17_05, CM17_06, and CM17_07.

All cores were driven into channel fill until refusal. Despite the use of core catchers, core recovery was less than desired. Core recovery, the percentage of core sample volume recovered after extraction, ranged from 24 to 40 percent (that is, 60–76 percent of the sediment column was not recovered as a result of either compaction during coring or loss; table 1). In sandy and pebbly deposits, compaction is expected to be minimal, but loss can be high because there are no cohesive sediments holding the core intact. The loss of sediment is likely the primary cause for the partial core recovery. Modification of the current core catcher design is needed to improve core recovery.

Interpretation of Sediment Cores

Four distinct deposits in the lower part of Corte Madera Creek were noted during field reconnaissance on July 18, 2017 (fig. 4). Layers generally appeared in the same order, from top to bottom. (1) Leaf litter and plant fragments were at the bed surface (numerous tree limbs were overhanging the concrete channel). (2) Pebbles, intermixed with sand, were just below the leaf litter in the concrete channel and on an intertidal bar just downstream from the concrete channel section. In most cases, this pebble layer appeared as a graded layer that could be further subdivided into layers of fine pebbles above medium pebbles, above coarse pebbles. (3) Clayey sand was both on shore-attached intertidal bars just downstream from the concrete channel and beneath the pebble layers. (4) Black mud was in the deeper parts of the earthen channel just downstream from the concrete channel and along the earthen levee bank.

The sediment in the cores was characterized by normally graded, sandy pebble deposits overlain by clayey sand (fig. 4). In the concrete channel section, leaf litter was found at the top of sediment cores. The normally graded, sandy pebble deposits were interpreted to have been deposited during wet-season watershed outflows. The clayey sand exhibited an erosive contact at the base of the units, which was interpreted to represent either sands deposited under lower tributary flows or reworked intertidal sand. The leaf litter was interpreted to have been deposited during dry-season, low-flow conditions.

In cores CM17_01 and CM17_07, black mud was beneath the normally graded sandy pebble deposits. Given the location of black mud in modern deposits, the fine-grained texture of the deposit, and the presence of invertebrate burrows in CM17_01, this deposit was interpreted to represent estuarine bay muds transported landward on flood tides and deposited during periods of decreased tidal flow speed.

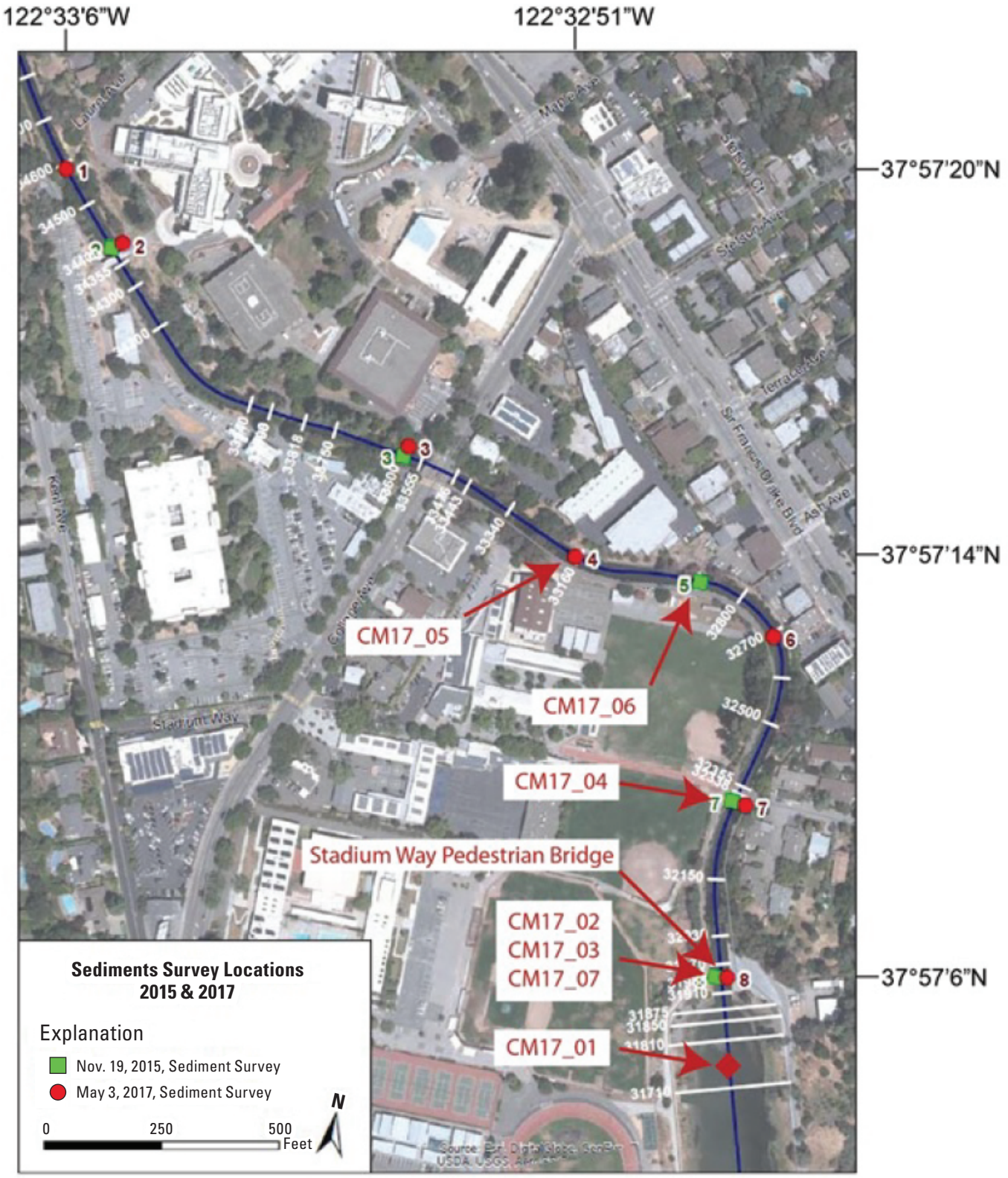

Figure 3. Coring and sediment survey locations on Corte Madera Creek, Marin County, California (Stetson Engineers, 2017, green boxes). Map modified from Stetson Engineers (2017). Station names beginning with CM are the designations used in this report. Core numbering is in chronological order.

Table 1. Summary of sediment cores collected August 24, 2017, on Corte Madera Creek, Marin County, California.

[Horizontal coordinates reference North American Datum of 1983 (NAD 83), elevations reference North American Vertical Datum of 1988 (NAVD 88). **Abbreviations**: ID, identification; —, not applicable (downstream from concrete channel section)]

Core ID	Latitude (degrees)	Longitude (degrees)	River station (feet)[1]	Core surface elevation (meter; NAVD88)[2]	Closest sediment elevation survey station[1]	Length recovered (meter)	Channel fill thickness (meters)[3]	Core recovery (percent)[4]	Maximum depth uncertainty (meter)[5]
CM17_01	37.9511	122.5455	31,760	–0.61	—	1.17	—	40	0.16
CM17_02	37.9517	122.5459	31,935	–0.80	8	0.55	1.81	30	0.07
CM17_03	37.9517	122.5459	31,935	–0.80	8	0.74	1.81	40	0.10
CM17_04	37.9527	122.5460	32,338	–0.97	7	0.23	0.88	24	0.01
CM17_05	37.9539	122.5474	33,160	–0.72	4	0.33	1.01	30	0.01
CM17_06	37.9539	122.5465	32,900	–0.41	5	0.42	1.24	35	0.01
CM17_07	37.9517	122.5459	31,935	–0.80	8	0.73	1.81	40	0.02

[1]Fields included for reference to previous work by U.S. Army Corps of Engineers (2016a) and Stetson Engineers (2017).

[2]Elevations from May 2017 survey except for CM17_01, which is from 2014.

[3]Channel-fill thickness computed from May 2017 sediment-elevation survey by Stetson Engineers (2017).

[4]The percentage of the undisturbed sediment retained in the coring tool after retrieval.

[5]Assumes either 15 or 30 degree tilt of core; see text.

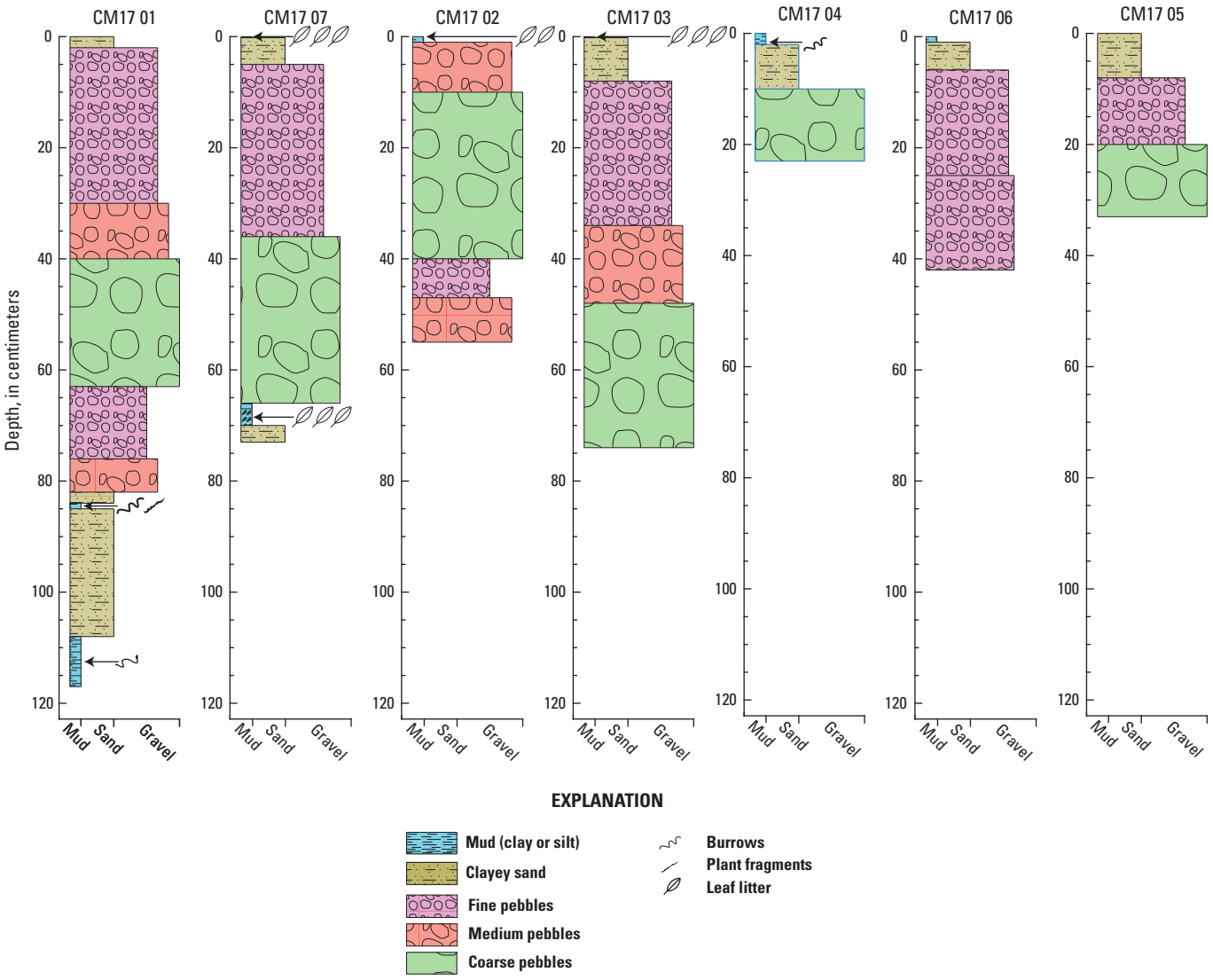

Figure 4. Descriptions of cores collected on August 24, 2017, by channel location (fig. 3) along Corte Madera Creek, Marin County, California. Left side of figure corresponds to downstream. Textural classifications for pebbles (fine, 2–8 mm; medium, 8–16 mm; and coarse, 16–64 mm) are based on Williams and others (2006).

Sediment Erosion and Deposition

A stratigraphic model using the available core descriptions was developed to test the two alternative depositional models of the channel fill. Collinson (1996) and Reading and Collinson (1996) provide stratigraphic models for alluvial deposits and estuarine deposits mixed with alluvial deposits, respectively. Using these stratigraphic models, two depositional models for the concrete channel section were considered. In the first, channel fill is flushed annually during each wet season, and the channel fill alluvial deposits are characterized by stacked, normally graded deposits (that is, deposits fine in the upward direction). These deposits thin in the seaward direction and abruptly terminate into estuarine muds at the channel terminus (fig. 2*A*; Collinson, 1996). In the second depositional model, where the channel aggrades episodically each wet season, the channel fill, alluvial deposits are characterized by numerous, nested, normally graded deposits interbedded with estuarine mud at the channel terminus (fig. 2*B*; Reading and Collinson, 1996). The cause of the interbedding of estuarine mud is landward transport of suspended sediments on flood tides, which settle during slack tide and are not re-suspended on subsequent ebb tides (van Straaten and Kuenen, 1958).

Channel bed elevation changes were computed from previous sediment surveys (Stetson Engineers on Nov. 19, 2015, the U.S. Army Corps of Engineers, or USACE, on April 4, 2016, and Stetson Engineers on May 3, 2017). From Nov. 19, 2015, to April 4, 2016, elevation change was less than 0.15 m at station 8, where core CM17_07 was collected. From April 4, 2016, to May 3, 2017, approximately 0.43 m of elevation gain was noted at this station. The observed bed elevation increase of 0.43 m is similar to the 0.66 m thickness of the pebbly deposit noted in the core at location CM17_07. Using the elevation survey from April 4, 2016, as representative of conditions after the wet period of WY2016 (fig. 5), a maximum of 0.23 m eroded at this site during WY2017 (fig. 6). The 3-cm thick leaf litter layer below the pebbly channel fill at location CM17_07 indicates that the channel fill was not completely reworked during wet-season watershed outflows at this location and that the peak WY2017 discharge of 129 cubic meters per second (m^3/s) (Station 11460000, Corte Madera Creek at Ross, Calif.) was not sufficient to scour all of the sediment from the concrete channel. The reported peak WY2017 discharge at this gage was slightly higher than 10-year peak discharge reported by the U.S. Army Corps of Engineers (2010; fig. 5).

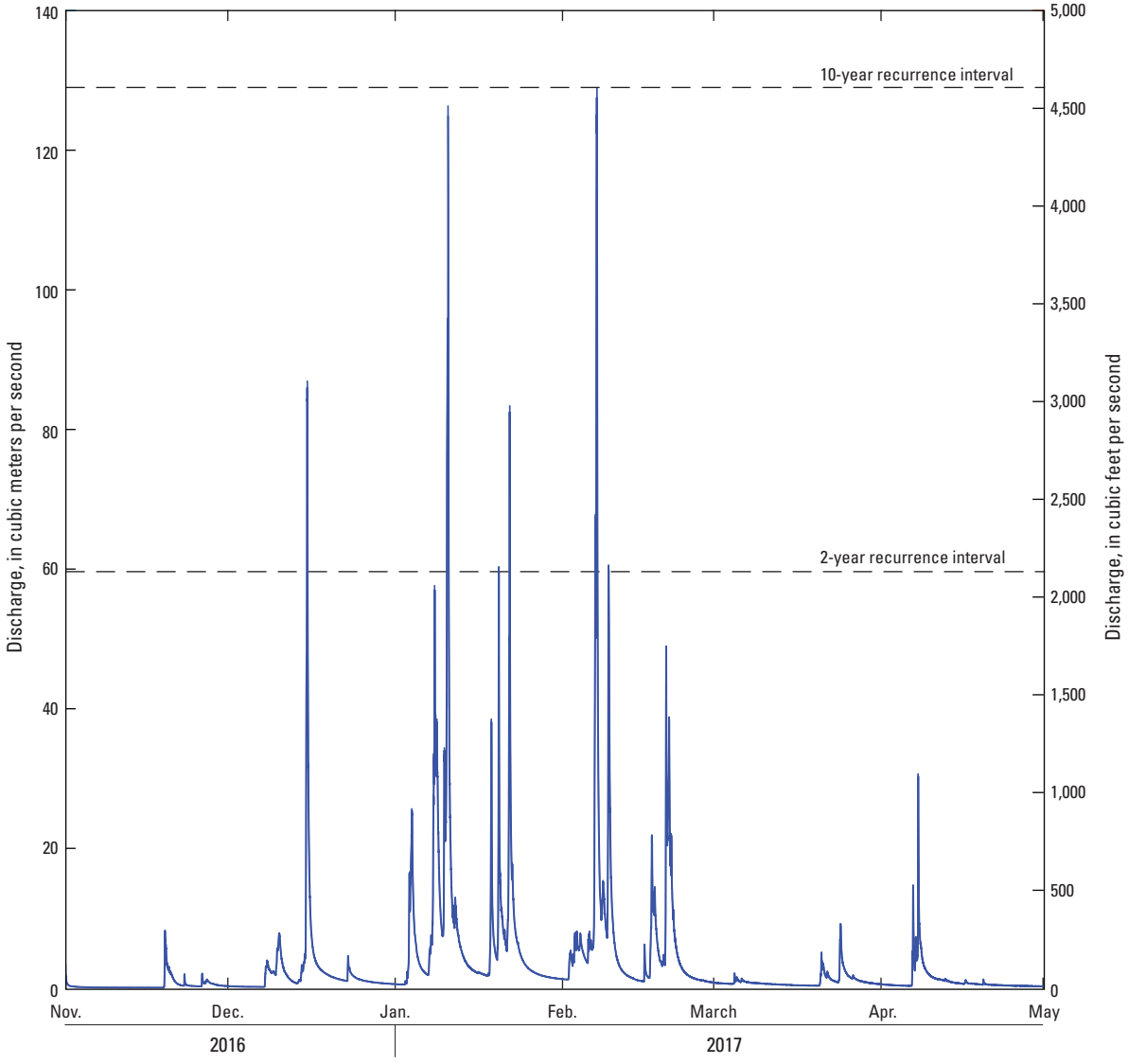

Figure 5. Part of water year 2017 hydrograph at U.S. Geological Survey gage 11460000, Corte Madera Creek at Ross, California. Discharges for 10- and 2-year return periods are from the U.S. Army Corps of Engineers (2010).

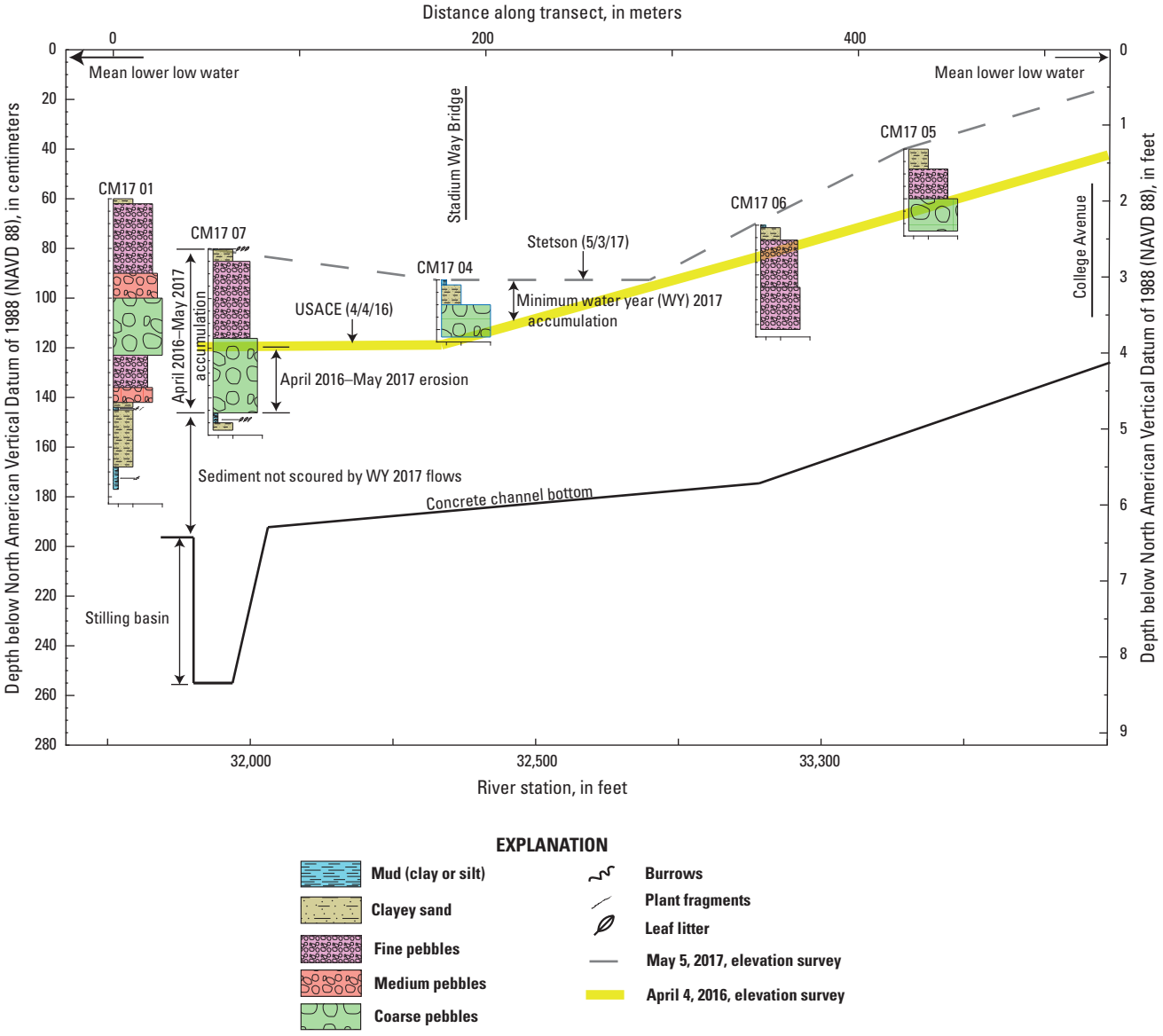

Figure 6. Core description by depth from bed sediment collected along a longitudinal transect of Corte Madera Creek, Marin County, California. Cores shown at coring locations; width of bar sections reflects relative grain size. Note, approximately 50 centimeters of channel fill was not scoured at CM17_07 during WY2017 flows.

Poor core recovery at stations CM17-04, 05, and 06 precluded more definitive assessment of which depositional model applies upstream from the settling basin. Studies from other watersheds that have mixed sand and gravel deposits, however, may be utilized to hypothesize whether scour increased or decreased upstream from station CM17_07. The critical shear stress for sediment in mixed sand and gravel beds is a function of coarse-particle exposure and absolute particle size (Dusterhoff and others, 2017, and references therein). Coarse-particle exposure is measured as the ratio of D_i to D_{50}, where D_i is the particle size (diameter) of the i^{th} percentile; for example, D_{84} is the diameter greater than 84 percent of the sample. Dusterhoff and others (2017) measured particle size and scour at four sites in western Marin County using scour chains to investigate how coarse-particle exposure affected maximum scour depth. Their work revealed that scour depth normalized by D_{90} was inversely proportional to the D_{84}/D_{50} ratio for sites that have similar D_{84} values but varying D_{50} values. Using their study and the particle size analysis of sediment collected by the U.S. Army Corps of Engineers (2016a) in April 2016, trends in erosion upstream from CM17_07 were inferred. Particle analysis of sediment collected before WY2017 was used because that was the sediment eroded by WY2017 flows. The U.S. Army Corps of Engineers (2016a) collected two samples in the concrete channel (table 2); one sample was collected at the end of the concrete channel, near core CM17_07, and another sample was collected upstream from the College Avenue Bridge near the upstream end of the channel fill (that is, upstream from station 3; fig. 3).

Table 2. Grain-size information derived from sieve analysis of material deposited on top of concrete channel bed. Samples collected in April 2016 on Corte Madera Creek, Marin County, California.

[Data from U.S. Army Corps of Engineers, 2016a. Horizontal coordinates are referenced to the North American Datum of 1983. **Abbreviation**: mm, millimeters; D, grain-size diameter; D_{xx}, where "xx" is the percentage of sample mass less than D]

Location	Latitude (degrees)	Longitude (degrees)	D_{50} (mm)	D_{84} (mm)	D_{84}/D_{50}	D_{90} (mm)
Upstream end of channel fill	37.9551	122.5513	4	17.6	4.4	20
Downstream end of channel fill	37.9517	122.5459	5	18.4	3.7	20

Based on the two samples shown in table 2, D_{50} increased from 4 to 5 mm downstream, and D_{84} increased from 17.6 to 18.4 mm. The net result is a slightly decreased D_{84}/D_{50} ratio, meaning decreased coarse-particle exposure downstream (table 2). These differences are small, however, and longitudinal gradients in shear stress applied to the bed by the gradually varying flow speeds and depths of the water above it are likely more important to the sediment transport potential.

The concept of a critical shear stress required for a flow to mobilize bed sediments is built into most investigations of bedload sediment transport. It is sometimes applied to the sediment bed, using only a representative sediment size, such as the median grain size. The Shields parameter is a dimensionless critical shear stress often used in this manner (see Mueller and others, 2005). Other approaches resolve the differences in critical shear stress for the different size fractions within the bed. Egiazaroff (1965) provides a theoretically derived equation to compute the dimensionless critical shear stress (τ^*_{ci}) in mixed sand and gravel systems that has been compared to field data from other published studies (Powell, 1998, fig. 4*A*):

$$\tau^*_{ci} = \frac{0.1}{\log_{10}\left(\frac{19D_i}{\bar{D}}\right)^2} \quad (1)$$

where

D_i is the grain size of the *i*th fraction, and
$\bar{D}$ is mean grain size.

Using median size, D_{50}, as an approximation of $\bar{D}$, one can compute the dimensionless critical shear stress and, thereby, the critical shear stress for the range of grain sizes observed in a channel. Dusterhoff and others (2017) observed variation in the relation between scour and bed shear stress for sites having different particle exposure but similar D_{84} values. This was attributed to increased coarse-particle exposure reducing the critical bed shear stress for the larger particles.

Equation 1 can be used to estimate critical shear stress to mobilize any size fraction from a sediment bed, given the mean size and a size of interest. Considering the two samples shown in table 2, however, the sizes and size distributions are similar enough to expect similar responses to similarly applied shear stresses. Expected temporal and longitudinal variation in applied shear stress is addressed in the next section.

Core descriptions do not clearly reveal longitudinal-channel trends in grain size (fig. 4). Grain size is typically expected to decrease exponentially with distance downstream, that is, $D = D_o e^{aL}$, where D is particle size, D_o is a reference particle size, a is a negative coefficient, and L is distance downstream from the reference site (Powell, 1998). The largest observed change in grain size along the longitudinal transect of the channel was at CM17_01, where gravel deposits transition into fine estuarine muds. This change is attributed to the widening of the channel and decreased channel slope and stream competency (ability to transport sediment) downstream from this point. In the concrete channel, shear stress frequently is sufficient to mobilize gravels until the channel widens and stream competency abruptly decreases. This hypothesis was investigated with the aid of a numerical model, as described in the next section.

One-Dimensional Simulation of Channel Flow and Bed Shear Stress

Although all flows in nature are three-dimensional, it is common to use two- or one-dimensional simulations when spatial variations in one or two directions are either insignificant or unimportant to the problem at hand. Flows in rivers are often simulated by one-dimensional models, neglecting the variations in the flow speed that can be observed across a flow cross section. Only longitudinal variations are resolved.

A one-dimensional simulation of flow in Corte Madera Creek was carried out to further investigate scour potential along the channel and longitudinal variations in flow speed and boundary shear stress. The model was used to simulate many different steady flow conditions, accounting for the backwater effect on water-surface profiles that arises when a flowing stream that has a modest slope reaches a water body in which water-surface height is effectively independent of the inflowing stream. If abrupt changes in flow conditions attributable to things like weirs and gates can be neglected, a steady (in time), gradually varied (in space) flow model can be used to resolve gradual changes in depth along the flow path. The model was written in Matlab® R2017a to solve coupled equations defining (1) conservation of mass and (2) conservation of energy (see, for example, Jain, 2001). The resulting code and input files are provided in Appendix 1 of this report.

The conservation of mass statement is this:

$$Q = UA = \text{Constant (for all locations, at a given time)} \quad (2)$$

where

Q is the volumetric discharge;
U is the mean flow speed at a given cross-section; and
A is the area of that cross-section, allowed to vary longitudinally to resolve actual channel geometry.

The energy equation, in its simplest form, is this:

$$\frac{dH}{dx} = -S_f \quad (3)$$

where

H is the hydraulic head (energy per unit weight);
x is distance along the channel bed in the direction of flow; and
S_f is the "friction slope" or energy loss per unit weight of water per unit length of channel, attributable primarily to channel bed and wall friction and energy dissipation caused by turbulence.

Typically, it is not possible to solve this pair of equations analytically, so they are combined and solved numerically. In this case, the equation to be solved becomes the following:

$$\frac{dy}{dx} = \frac{S - S_f}{1 - Fr^2} \quad (4)$$

where

$$Fr = \frac{U}{\sqrt{gD}} \quad (5)$$

y is water depth,
S is channel bed slope,
Fr is Froude number,
g is the acceleration due to gravity, and
D is the hydraulic depth (the ratio of flow cross-sectional area to width of the water surface in the channel).

The basic approach of this model is like that of the US Army Corps of Engineers' HEC-RAS model (U.S. Army Corps of Engineers, 2016b), when run in one-dimensional mode.

Equation (4) is an ordinary differential equation, and there are different ways to solve it numerically. The code utilized here provides options for Euler, improved Euler, modified Euler, Runge-Kutta 4th, and iterative Newton-Raphson solutions; Euler method was used here. All use the same input data. If longitudinal step size is specified as input, all represent "Standard Step" solution options.

For subcritical flow (Fr less than 1), which is the most common scenario in nature, one starts from a known or assumed water depth at the downstream end of the model domain (for example, tide level in the receiving bay) and performs calculations working upstream. This was the approach here, using varying discharges and varying downstream water levels. Channel width, elevation, and roughness are from the U.S. Army Corps of Engineers (1989). Discharge values were chosen to range from 1 m^3/s to the peak WY2017 discharge of 129 m^3/s at 4–20 m^3/s intervals (figs. 7–8). Downstream water levels were chosen at 0.1-m intervals from mean lower low water to mean higher high water (MHHW) for each discharge value. The upstream end of the model domain is at the USGS Ross gage (NWIS ID: 11460000) and the downstream end at the Corte Madera Creek NOAA tide gage (Station ID: 9414874). Overtopping of the channel sidewalls was not considered in the model.

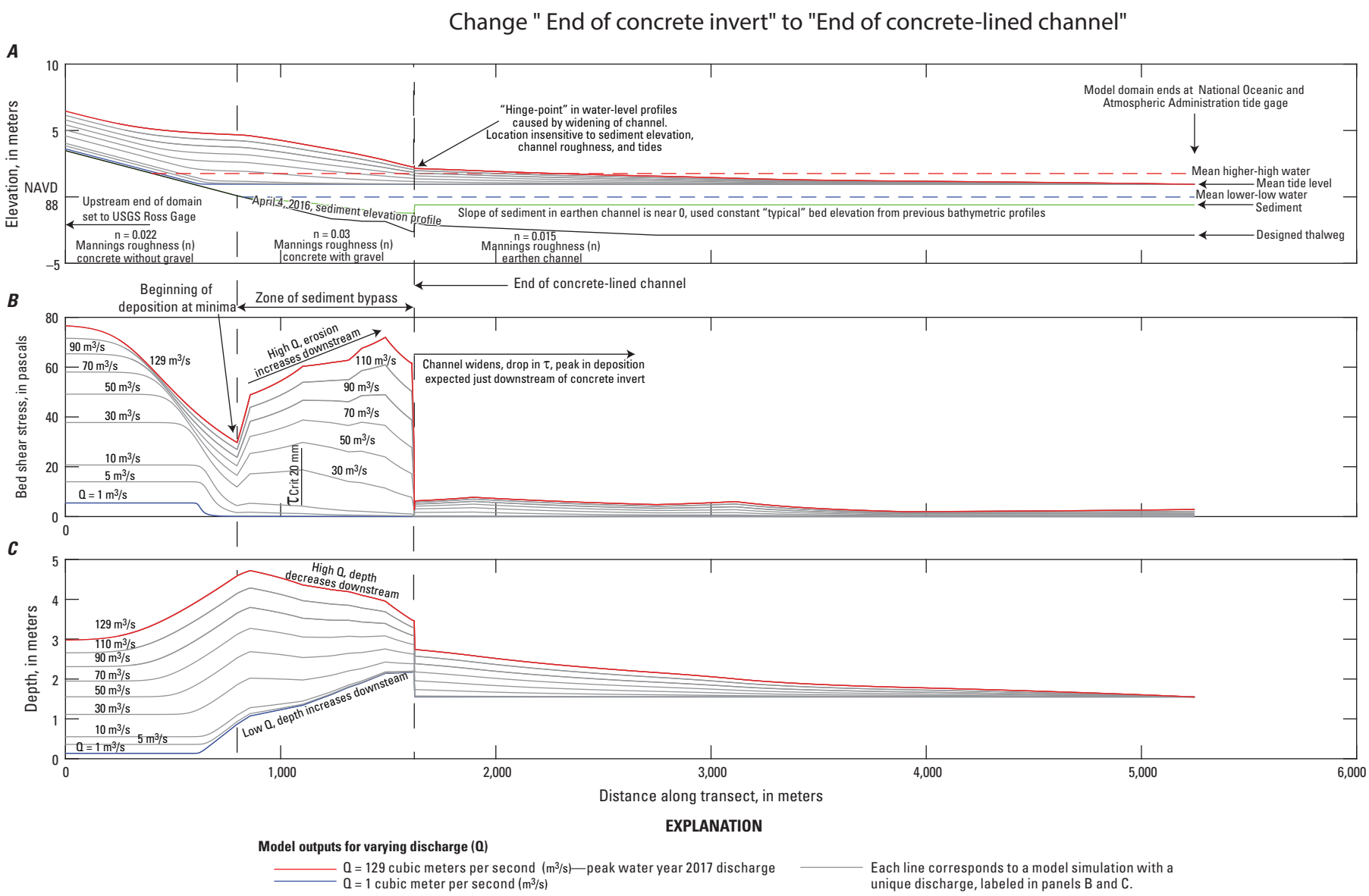

Figure 7. One-dimensional hydrodynamic model results for Lower Corte Madera Creek, California, that account for backwater effect on water-surface profiles. Upstream end of domain is at left. Note that results for discharge, Q, of 129 m³/s, shown by the red curves, represent the largest observed discharge in water year 2017 and slightly exceed the 10-yr peak discharge reported by U.S. Army Corps of Engineers (2010). *A*, Water-surface profiles for different flow rates with downstream control at mean tide level (MTL). *B*, Bed shear stress as function of distance along channel. τcrit_20mm is of critical shear stress for 20-millimeter (mm) particles; range of values estimated using Shields equation and range of Shields parameters from Mueller and others (2005). *C*, Water depth along the channel. mm, millimeter; NAVD 88, North American Vertical Datum of 1988.

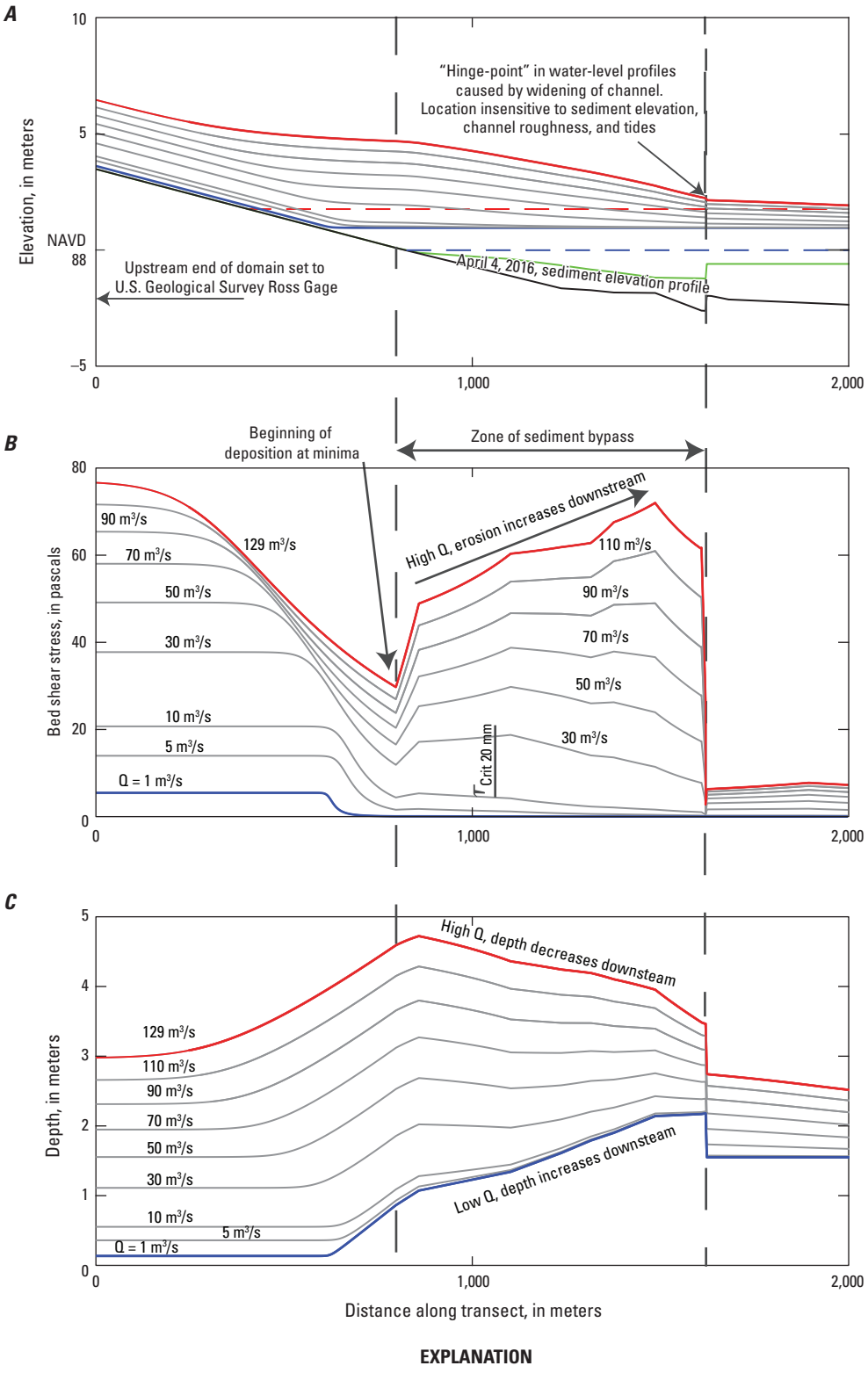

Figure 8. Detail of figure 7 showing simulation results for upstream end of model domain, Corte Madera Creek, California: *A*, water-surface profiles for different flow-rate scenarios; *B,* bed shear stress as function of distance along channel; *C,* water depth along the channel. m³/s, cubic meter per second; mm, millimeter; NAVD 88, North American Vertical Datum of 1988.

One must evaluate the friction slope to fully develop the model. One form of the Manning equation, originally developed to describe uniform, steady flow in open channels or rivers, is as follows:

$$Q = \frac{C}{n} AR^{2/3} S^{1/2} \quad (6)$$

where

Q is channel discharge, volume per unit time;
C takes the value 1.0 for International System (SI) units (used here) or 1.49 for the foot-pound-second (fps) system of units;
n is the Manning roughness coefficient;
A is the flow cross-sectional area;
R is the hydraulic radius, ratio of channel cross-sectional area to wetted perimeter; and
S is the slope of bed surface in longitudinal direction.

Strictly speaking, the Manning roughness coefficient is dimensional and, therefore, should have different values for the SI and fps unit systems. In practice, however, the value for C defined before is used to do the conversion in unit systems, and n is treated as dimensionless, taking the same values in both unit systems (Jain, 2001; Sturm, 2001). Manning's n was treated as dimensionless throughout this report.

The friction slope was evaluated by replacing the bed-slope term by the friction slope in the Manning equation and solving for the friction slope S_f:

$$S_f = \frac{nQ}{CAR^{2/3}} = \frac{nU}{CR^{2/3}} \quad (7)$$

Thus, as flow speed increases or depth decreases, the rate of energy dissipation, as given by the friction slope, increases.

Manning's roughness friction factors for the concrete channel were from a HEC-RAS model calibration by U.S. Army Corps of Engineers (1989). Values of 0.022, 0.030, and 0.015 were assigned to the concrete channel lacking gravel, the concrete channel with gravel, and the earthen levee, respectively (U.S. Army Corps of Engineers, 1989). The transition in channel geometry, in this case, was resolved in the model, but its abruptness was not. In reality, the energy loss at the transition would be greater than what was simulated in the model, which means upstream water levels would be slightly higher than simulated. Nevertheless, the results are useful for interpretation and show the trends in bed shear stress along the channel and as the tide changes downstream boundary conditions.

Shear stress (τ) along the channel bed can be related to the hydraulic radius R and bed slope S using equation 8 (Jain, 2001):

$$\tau = \rho g R S \quad (8)$$

where

ρ is the density of water (mass per volume), and
g is acceleration due to gravity.

Unlike the dimensionless critical shear stress τ^*_{ci}, bed shear stress τ is dimensional and, for this study, is reported using the SI unit, pascal, equivalent to newtons per square meter (N/m^2).

Model results are shown in figures 7 and 8. Each figure shows the water-surface profile above the modeled channel geometry in the top panel, followed by plots of shear stress and water depth in the lower panels. Depth and shear stress change abruptly near the mean tide level and at the end of the concrete channel section, where channel cross-section changes abruptly. The two plotted results that featured the largest flow rates show depths great enough to overtop the concrete channel sidewalls near where x is equal to 1000 m, and the sponsor of this work noted that overtopping was observed during the peak flow of WY2017 (the maximum flow simulated). As noted earlier, overtopping was not included in the model, but most of the simulated cases featured no overtopping, and the suite of model results is useful for the primarily qualitative way in which they were used.

The model results indicate that for the higher simulated discharges, bed shear stress decreased in the downstream direction until the point where the bed elevation was close to the mean lower low water (MLLW) elevation. Beyond this point, bed shear stress increased at increasing distance downstream, until the point where the channel widened and bed shear stress dropped sharply. In figures 7 and 8, the peak flow of WY2017 is shown by a red line. This peak discharge slightly exceeded that for the 10-year return period (10-percent annual chance of exceedance). The peak discharge corresponding to the 2-year event was approximately 60 m^3/s, in the middle of the range of simulated discharges (U.S. Army Corps of Engineers, 2010).

A range of critical shear stress values for the reported value of D_{90} at the site (20 mm) was estimated using the Shields equation (see U.S. Army Corps of Engineers, 1989) and a range of observed critical Shields parameters published for bedload sediment transport (Mueller and others, 2005). The results are superimposed as a short vertical line on figures 7*B* and 8*B*. It is evident in the figures that only the lower discharges (less than 50 m^3/s) were likely to result in deposition of these large classes of sediment in the narrow parts of the channel. Downstream from the abrupt widening of the channel, velocity and bed shear stress both dropped sharply, and sediment deposition would be expected in this zone.

Very low discharges (less than 10 m^3/s) led to very low bed shear stresses in the region just upstream from the widening of the channel. As a result, in this region, which lies just below MLLW but is upstream from the widening of the channel, model results indicated occasional sedimentation, with episodic scouring during higher flows, whereas the region farthest downstream would be expected to exhibit deposition during all flow conditions within the simulated range.

Survey data were consistent with these conclusions. Four sediment elevation surveys from the concrete channel region indicated that the deposited sediment was typically found below the mean lower low water (MLLW) elevation (Stetson Engineers, 2017). As the flow passing through the channel varied in time, its ability to transport sediment of different size classes changed, but unless very low discharges were encountered, bed shear stress remained high enough to transport most of the sediment load to the region below the MLLW. A coupled hydrodynamic-sediment transport model that resolves size-specific sediment transport would be needed to estimate the total longitudinal scour and deposition along the channel expected for any particular hydrological scenario.

Conclusions

Sediment cores, stratigraphy, sediment elevation profiles, grain-size data, and a one-dimensional hydrodynamic model were utilized to investigate longitudinal sediment deposition and scour along the channel following the wet season of WY2017, focusing on the intertidal part of the concrete channel section of Corte Madera Creek. Sedimentation in a channel can reduce flood conveyance and place property and life at risk from flooding. This study was limited in scope but, by combining field observations and numerical modeling, revealed sedimentation patterns for conditions ranging from very low spring and summer flows up to high flows with recurring intervals exceeding 10-years.

The goal of this work was to test two alternative hypotheses describing sediment deposition in the concrete channel: (1) complete flushing during and subsequent re-deposition of channel fill after high-flow events or (2) more steady, gradual channel infilling. Determining how and when this material was deposited informs dredging operations for the Corte Madera Creek Flood Control Project and increases understanding of sediment delivery timing and mechanisms for the site. Findings of this study include the following:

1. Analysis of the sediment cores revealed that the storm flows of 2017, one of which slightly surpassed the 10-year discharge at the U.S. Geological Survey gage at Ross, upstream from the site, did not completely scour the concrete channel fill, and the channel is gradually infilling. Sediment cores, stratigraphic analysis, and sediment elevation profiles indicated 0.23 meter (m) was scoured at the downstream end of the concrete-lined section and that roughly 0.5 m of channel fill remained in the channel.

2. The hydrodynamic model indicated that during low-flow events, a negative shear stress gradient in the intratidal part of the concrete-lined section was conducive to sediment deposition. High-flows led to much higher bed shear stresses and a positive downstream gradient in this reach, which was conducive to scour. A coupled hydrodynamic-sediment transport model would be needed to quantify expected total scour volumes along the channel expected during a given period. A careful estimate of the in situ critical shear stress for erosion of sediment deposits having particle size distribution similar to the mixture of sand, pebbles, and cobbles observed in this and previous studies would also be needed.

3. The hydrodynamic model demonstrated that sediment deposition in the concrete channel is expected to start downstream from the point where the channel bed reaches mean lower low water (MLLW) level. High flows can carry most of the sediment through this section of channel, with deposition downstream from the transition to a wide channel where flow speed and bed shear stress decrease abruptly.

Although the storms of 2017 did not completely scour the channel fill, subsequent material deposited in the channel could be transported downstream from the concrete channel if the sediment elevation profile was in equilibrium with current mean sea level. Additional work using a coupled hydrodynamic-sediment transport model could determine whether sediment elevation profiles are in equilibrium with mean sea level, such that additional sediment build-up in the concrete channel would be mobilized downstream from the concrete channel during subsequent wet-season flows.

References Cited

Collinson, J.D., 1996, Alluvial sediments, chap. 3 *of* Reading, H.G., ed., Sedimentary environments—Processes, facies and stratigraphy (3rd ed.): Oxford, Blackwell Science, p. 37–82.

Dusterhoff, S.R., Sloat, M.R., and Ligon, F.K., 2017, The influence of coarse particle mobility on scour depth in salmonid spawning habitat: River Research and Applications, v. 33, no. 8, p. 1306–1314.

Egiazaroff, I.V., 1965, Calculation of nonuniform sediment concentrations: Journal of the Hydraulics Division, v. 91, no. 4, p. 225–247.

Jain, S.C., 2001, Open-channel flow: New York, John Wiley and Sons, 328 p.

Kamman, 2014, Hydraulic assessment of existing conditions Novato Creek Watershed Project: Kamman Hydrology & Engineering, Inc., San Rafael, CA, 198 p., http://www.marinwatersheds.org/sites/default/files/2018-04/3109_NovatoCr_EC_FINAL_140630_sm.pdf.

Mueller, E.R., Pitlick, J., and Nelson, J.M., 2005, Variation in the reference Shields stress for bed load transport in gravel-bed streams and rivers: Water Resources Research, v. 41, no. 4, 10 p.

Powell, D.M., 1998, Patterns and processes of sediment sorting in gravel-bed rivers: Progress in Physical Geography, v. 22, no. 1, p. 1–32.

Reading, H.G., and Collinson, J.D., 1996, Clastic coasts, chap. 6 *of* Reading, H.G., ed., Sedimentary environments—Processes, facies and stratigraphy (3rd ed.): Oxford, Blackwell Science, p. 154–231.

Stetson Engineers, 2000, Geomorphic assessment of the Corte Madera Creek Watershed: Stetson Engineers Inc., San Rafael, CA, 91 p., http://www.krisweb.com/biblio/nsfb_fcmc_stetsoninc_2000_geomorph.pdf.

Stetson Engineers, 2017, May 2017 Sediment measurements and comparison with November 2015 sediment measurements in the Corte Madera Creek Concrete Channel: Stetson Engineers, Inc., San Rafael, CA, 9 p., http://marinwatersheds.org/sites/default/files/2018-02/Sediment%20Comparison%20Memo%202015-2017.pdf.

Sturm, T.W., 2001, Open channel hydraulics: Boston, McGraw-Hill, 493 p.

U.S. Army Corps of Engineers, 1989, Corte Madera Creek sedimentation study: Numerical Model Investigation, 79 p., available online at https://apps.dtic.mil/dtic/tr/fulltext/u2/a207175.pdf.

U.S. Army Corps of Engineers, 2010, Corte Madera Creek flood control study baseline report: U.S. Army Corps of Engineers San Francisco District, 178 p., available online at http://www.marinwatersheds.org/sites/default/files/2017-11/CorteMaderaCreekFinalBaselineReport-2010-12-08_0.pdf.

U.S. Army Corps of Engineers, 2016a, Sediment sampling on Corte Madera creek to inform sediment deposition depths and sediment grain size distribution: U.S. Army Corps of Engineers, San Francisco District, Memorandum of Record, April 5, 2016.

U.S. Army Corps of Engineers, 2016b, HEC-RAS River Analysis System users manual, v. 5.0, CPD-68: Institute for Water Resources, Hydrologic Engineering Center, Davis, CA, 960 p.

van Straaten, L.M.J.U., and Kuenen, P.H., 1958, Tidal action as a cause of clay accumulation: Journal of Sedimentary Petrology, v. 28, no. 4, p. 406–413.

Wentworth, C.K., 1922, A scale of grade and class terms for clastic sediments: The Journal of Geology, v. 30, no. 5, p. 377–392.

Williams, S.J., Arsenault, M.A., Buczkowski, B.J., Reid, J.A., Flocks, J.G., Kulp, M.A., Penland, S., and Jenkins, C.J., 2006, Surficial sediment character of the Louisiana offshore Continental Shelf region—A GIS Compilation: U.S. Geological Survey Open–File Report 2006–1195, 49 p., available online at https://doi.org/10.3133/ofr20061195.

Appendix 1. One-Dimensional Model for Surface Water Elevation Profiles Using the Standard Step Method

A Matlab© R2017a function was written to compute water-surface profiles using the Standard Step Method. It is named StandardCM.m. It is called by a script named CorteMaderaLoop.m that prepares input for the function and plots results. Two input files define the elevations of water levels of interest and the geometry of the channel at the Corte Madera site. These are ASCII files named Tide.txt and CMGeom.txt, respectively. All four files are reproduced here.

File: CorteMaderaLoop.m

```
% This file clears memory, defines model input, and calls model
% for each case of interest. Model is contained in file StandardCM.m
% variables are defined there.

clear

% load in channel geometry data. Columns contain:
% station location in ft (decreases in downstream direction)
% elevation of bed, m NAVD 88
% bed elevation survey, May 2017
% bed elevation survey, April 2016
% channel bottom width, m
% channel side slope (run over rise)
% Manning's n
CM_Geometry_mNAVD88=readtable('CMGeom');

% load in tide datum info
Tide=readtable('Tide');

% Corte Madera Creek 1D hydrodynamic model, model from P. Work
% CM_Geometry_mNAVD88 channel geometries USACE w/gravel surveys from Stetson
% Tide - Tidal datums from USACE relative to NAVD88
% Model domain from Ross Gage to US 101 Bridge, elevation of bed from end
% of concrete channel to US 101 bridge varies but very little, assumed
% "characteristic" channel depth downstream of concrete channel from
% Stetson bed elevation surveys

G = CM_Geometry_mNAVD88;
```

```
% Compute xi, mann, and zchan
% River stations for x (increase upstream). Ross gage is upstream point
Station = G.Stationft;

% meters increasing downstream from River Station (ft) 37214 (1 mile up from end of concrete channel)
xS = round((Station(1)-Station).*0.3048,0); % distance of surveyed stations downstream of Ross gage, in
m
Bed = G.ElevatonofbedmNAVD88; % bed elevation
Gravel = G.Apr2016mNAVD88; % elevation in Apr 2016 survey
% Interpolate bed onto dx for computation
xi = 0:0.25:max(xS); % 0.25 m horizontal step

% Compute parameters along channel at fine dx
zchan = interp1(xS,Gravel,xi,'linear'); % channel bed elevation
mann = interp1(xS,G.manningsn,xi,'linear'); % manning's n
bo = interp1(xS,G.wm,xi,'linear'); % channel bottom width
sslope = interp1(xS,G.Sidesloperunrise,xi,'linear'); % side slope
% end of channel at 31900 (1620 m from upstream limit)
bslope(xi>1620) = 0; % Run/Rise
sslope(xi>1620) = 6/1; % Run/Rise


%% Compute profile with different values of Q (fig. in report)

Qi = [1 5 10:20:110 129]; % Qs USED IN report, 129 m3/s was peak WY 17 Q at Ross
color = {'k','g','b','r'};
grav = 9.81; % acceleration of gravity
alp = 1; % energy coefficient
flag = 1; % controls solution method
baselevel = Tide.MTL-zchan(end); % baselevel can be varied; this is d/s depth

close
clear param* CritRange param*
for j = 1:length(Qi) % loop to do calcs for each discharge
   Q = Qi(j);
for i = 1:length(baselevel) % loop to do calcs for each water level
   y1 = baselevel(i);
% Ross gauge is ~ 1 mile upstream of concrete channel terminus (Station 37950)
```

```
% Datum of Ross gage is 7.97 ft above NGVD of 1929). NGVD29 is ~ 2.72 ft below
% NAVD88.
end

% flip input vectors as need be; first value must be downstream for
% subcritical flow
[paramSub]=StandardCM(flip(xi),flip(zchan),y1,Q,flip(bo),flip(sslope),flip(mann),alp,grav,flag,0); hold on

figure(1)
fig1=figure(1); % ensures figure is vectorized when exported to pdf
fig1.Renderer='Painters'; % ensures figure is vectorized when exported to pdf
h3 = subplot(3,1,3);
% yyaxis left
plot(paramSub.x,paramSub.Depth,'color',[0.5 0.5 0.5]),hold all
set(gca,'FontSize',12)
if Q == min(Qi)
plot(paramSub.x,paramSub.Depth,'b'),hold all
end
if Q == max(Qi)
plot(paramSub.x,paramSub.Depth,'r'),hold all
end
ylabel('Depth (m)')
xlabel('Distance along transect (m)')

h2 = subplot(3,1,2);
plot(paramSub.x,paramSub.tau,'color',[0.5 0.5 0.5]),hold all
if Q == min(Qi)
plot(paramSub.x,paramSub.tau,'b'),hold all
end

if Q == max(Qi)
plot(paramSub.x,paramSub.tau,'r'),hold all
end
ylabel('\tau (N/m^2)')

h1 = subplot(3,1,1);
```

```
plot(paramSub.x,paramSub.Depth+paramSub.BedElev,'color',[0.5 0.5 0.5])
ylabel('Elevation (m, NAVD88)')
set(gca,'FontSize',12)
if Q == min(Qi)
plot(paramSub.x,paramSub.Depth+paramSub.BedElev,'b'),hold all
end
%
if Q == max(Qi)
plot(paramSub.x,paramSub.Depth+paramSub.BedElev,'r'),hold all
plot(paramSub.x,paramSub.BedElev,'g'),hold all
end

end



plot(xS,Gravel,'g-')
plot(xS,Bed,'k')
% plot(xS,Wall,'k')
plot([825 max(xS)],[Tide.MLLW Tide.MLLW],'b--')
plot([400 max(xS)],[Tide.MHHW Tide.MHHW],'r--')
set(gca,'FontSize',12)
linkaxes([h1 h2 h3],'x')
```

File: StandardCM.m

```
function [param]=StandardCM(x,zchan,y1,Q,bo,sslope,mann,alp,grav,flag,pflag)

% Modified from standard.m written by Paul A. Work (USGS California
% Water Science Center) to solve steady, gradually varied flow
% problems (1-D) by standard step method.

% This is covered in most open-channel flow books. One reference:
% Jain, S.C., 2001. Open-Channel Flow, Wiley.

% Each model simulation requires channel geometry information, a
% discharge, and a controlling water depth. For subcritical flows,
% this must be a depth at the downstream end of the domain, and
% calculations proceed upstream. For supercritical flows, an upstream
```

```
% depth must be provided, and calculations proceed downstream.
% If a transition between the two occurs, one must patch together
% two solutions. For the cases considered here, though, only
% subcritical conditions were encountered.

% D.N. Livsey (USGS CAWSC) modified outputs and added some calcs
% to customize the code for Corte Madera Creek. Input data are
% read in from external files when this code is executed.

% A trapezoidal channel is assumed.
% Definitions of variables:
% x = vector of x-positions at which depths will be computed.
% x increases going downstream.
% ystand = computed water depths. Size matches that of x.
% If subcritical flow, first x-value in array should correspond
% to downstream limit, then get smaller. If supercritical, should start
% at upstream limit and get larger.
% zchan = corresponding vector of channel bottom elevations,
% with same ordering requirements as x
% y1 = control depth (specified by user). d/s end if subcritical,
% u/s end if supercritical.
% Q = volumetric flowrate
% bo = bottom width, corresponding vector of channel widths
% sslope = sideslope (rise/run) corresponding vector of sideslopes
% mann = Manning's n, corresponding vector of channel roughness
% alp = velocity coefficient, alpha; typically 1.0 if not otherwise known
% grav = acceleration of gravity
% area?,perim?,top?,hydr? = flow area, wetted perim, top width, and
%                           hydraulic radius at section ?. 1=d/s.
% y2=u/s depth
% fy2 = function for Newton-Raphson solution
% dfdy2 = derivative of above function
% tol = tolerance in Newton-Raphson loop
% itmax = max number of iterations
% flag can assume the following values
% "Open Channel Flow")
% 0 yields Euler solution
```

```
% 1 yields improved Euler solution
% 2 yields modified Euler solution
% 3 yields Runge-Kutta 4th order solution
% 4 yields Newton-Raphson iterative solution
% pflag: plotting option 0 = NO, 1 = YES

% Information on input files:
% CMGeom channel geometries USACE w/ gravel surveys from Stetson
% RossGageData - USGS Ross Stage (Discharge) rating
% CMTide - Tidal datums from USACE relative to NAVD88
% Model domain extends from Ross Gauge to US 101 Bridge, elevation of
% bed from end of concrete channel to US 101 bridge varies but very
% little, assumed "characteristic" channel depth downstream of concrete
% channel from Stetson Engineers bed elevation surveys

tol=0.00001;
itmax=100;
imax=max(size(x));
ystand(1:imax)=NaN;
ystand(1)=y1;

% DNL modified PAW's code to output 'Param' table with inputs and outputs
% param = table(x',ystand',zchan',area,perim,R,Uxs,Cd,tau);
% param.Properties.VariableNames = {'x','Depth','BedElev','Area','Perimeter','R','Uxs','Cd','tau'};
% Derived Cd from manningn n using t = yRS, t = 0.5*p*Cd*u2, and
% u = (1/n)*R^(2/3)*s^0.5

% Preallocate output variables
area = NaN(max(size(x)),1); % Cross-sectional area
perim = NaN(max(size(x)),1); % Wetted perimeter
R = NaN(max(size(x)),1); % Hydraulic Radius
Uxs = NaN(max(size(x)),1); % Mean cross section velocity


for i=1:imax-1

% Calculate head at downstream end
```

```
area1=bo(i)*y1+sslope(i)*y1^2;
head1=zchan(i)+y1+alp*Q^2/(2*grav*area1^2);
slope=-(zchan(i+1)-zchan(i))/(x(i+1)-x(i));


% Calculate friction slope; use this to estimate depth at next point u/s
C=1.49;
if grav<30
C=1.0;
end
perim1=bo(i)+2*y1*sqrt(1+sslope(i)^2);
hydr1=area1/perim1;
top1=bo(i)+2*sslope(i)*y1;
Sf1=(mann(i)*Q/(C*area1*hydr1^(2/3)))^2;
fxy=(slope-Sf1)/(1-alp*top1*Q^2/(grav*area1^3));

% check to make sure that flow regime matches input, i.e.
% if subcritical, start at downstream end and march upstream,
% or vice-versa
Fr1=Q/area1/sqrt(grav*top1);
if (x(1)>x(imax) && Fr1>1)
   x(i)
   Fr1crit = Fr1;
   disp('Error: cannot start at downstream end if supercritical; stopping')
   break
elseif(x(1)<x(imax) && Fr1<1)
   x(i);
   Fr1Sub = Fr1;
   disp('Error: cannot start at upstream end if subcritical; stopping')
   break
end

% This is initial guess for y2; corresponds to Euler method
y2=y1+fxy*(x(i+1)-x(i));
area2=bo(i)*y2+sslope(i)*y2^2;
perim2=bo(i)+2*y2*sqrt(1+sslope(i)^2);
hydr2=area2/perim2;
```

```
top2=bo(i)+2*sslope(i)*y2;
Sf2=(mann(i)*Q/(C*area2*hydr2^(2/3)))^2;
fxy2=(slope-Sf2)/(1-alp*top2*Q^2/(grav*area2^3));

% now do calculations for improved Euler method
if flag==1
  y2=y1+1/2*(fxy+fxy2)*(x(i+1)-x(i));
% or modified Euler method
elseif flag==2
  y2=y1+fxy*1/2*(x(i+1)-x(i));
  area2=bo(i)*y2+sslope(i)*y2^2;
  perim2=bo(i)+2*y2*sqrt(1+sslope(i)^2);
  hydr2=area2/perim2;
  top2=bo(i)+2*sslope(i)*y2;
  Sf2=(mann(i)*Q/(C*area2*hydr2^(2/3)))^2;
  fxy=(slope-Sf2)/(1-alp*top2*Q^2/(grav*area2^3));
  y2=y1+fxy*(x(i+1)-x(i));
% or Runge-Kutta 4th order solution
elseif flag==3
  k1=fxy;
  y2=y1+1/2*k1*(x(i+1)-x(i));
  area2=bo(i)*y2+sslope(i)*y2^2;
  perim2=bo(i)+2*y2*sqrt(1+sslope(i)^2);
  hydr2=area2/perim2;
  top2=bo(i)+2*sslope(i)*y2;
  Sf2=(mann(i)*Q/(C*area2*hydr2^(2/3)))^2;
  fxy2=(slope-Sf2)/(1-alp*top2*Q^2/(grav*area2^3));
  k2=fxy2;
  y2=y1+1/2*k2*(x(i+1)-x(i));
  area2=bo(i)*y2+sslope(i)*y2^2;
  perim2=bo(i)+2*y2*sqrt(1+sslope(i)^2);
  hydr2=area2/perim2;
  top2=bo(i)+2*sslope(i)*y2;
  Sf2=(mann(i)*Q/(C*area2*hydr2^(2/3)))^2;
  fxy2=(slope-Sf2)/(1-alp*top2*Q^2/(grav*area2^3));
  k3=fxy2;
  y2=y1+k3*(x(i+1)-x(i));
```

```
  area2=bo(i)*y2+sslope(i)*y2^2;
  perim2=bo(i)+2*y2*sqrt(1+sslope(i)^2);
  hydr2=area2/perim2;
  top2=bo(i)+2*sslope(i)*y2;
  Sf2=(mann(i)*Q/(C*area2*hydr2^(2/3)))^2;
  fxy2=(slope-Sf2)/(1-alp*top2*Q^2/(grav*area2^3));
  k4=fxy2;
  y2=y1+1/6*(k1+2*k2+2*k3+k4)*(x(i+1)-x(i));
% or Newton-Raphson iterative solution
elseif flag==4
% Start Newton-Raphson loop to calculate y2
  for k=1:itmax
  area2=bo(i)*y2+sslope(i)*y2^2;
  perim2=bo(i)+2*y2*sqrt(1+sslope(i)^2);
  hydr2=area2/perim2;
  top2=bo(i)+2*sslope(i)*y2;
  Sf2=(mann(i)*Q/(C*area2*hydr2^(2/3)))^2;
  fy2=y2+alp*Q^2/(2*grav*area2^2)+1/2*Sf2*(x(i+1)-x(i))+zchan(i+1)-head1+1/2*Sf1*(x(i+1)-x(i));
  dR2dy2=top2/perim2-area2/perim2^2*2*sqrt(1+sslope(i)^2);
  dfdy2=1-alp*Q^2*top2/(grav*area2^3)-(x(i+1)-x(i))*(Sf2*top2/area2+2/3*Sf2/hydr2*dR2dy2);
  y2=y2-fy2/dfdy2;
  if abs(fy2/dfdy2)<tol
    if k>10
      k
    end
    break
  end
  end
end

if flag == 0
if i == 1
area(i) = area1;
perim(i) = perim1;
end
area(i+1) = area1;
perim(i+1) = perim1;
```

```
end

if flag > 0
if i == 1
area(i) = area2;
perim(i) = perim2;
end
area(i+1) = area2;
perim(i+1) = perim2;
end



ystand(i+1)=y2;
% check Froude Numbers, using hydraulic depth for depth scale
Fr1=(Q/area1)/(sqrt(grav*(area1/top1)));
Fr2=(Q/area2)/(sqrt(grav*(area2/top2)));
if (Fr1<=1 && Fr2>1 && y2>0)
display(strcat('Change from sub to supercritical at i=',num2str(i)))
break
elseif (Fr1>1 && Fr2<1 && y2>0) % (Fr1>1 && Fr2<=1 && y2>0) PAW's condition
Q
display(strcat('Change from super to subcritical at i=',num2str(i)))
break
end

y1=y2;
end



% get rid of complex (invalid) results
for i=2:imax
if (~isreal(ystand(i)) || ystand(i)<0)
   ystand(i)=NaN;
```

```
end

end

% Compute R and Uxs
R = area./perim; % Hydrauic Radius
Uxs = Q./area; % Mean cross section velocity
% Derive Cd from manningn n using t = yRS, t = 0.5*p*Cd*u2, and
% u = (1/n)*R^(2/3)*s^0.5
Cd = ((2.*grav.*mann.^2)./R'.^(1/3))';
tau = 0.5.*1000.*Cd.*(Uxs.^2);

% Store output parameters
param = table(x',ystand',zchan',area,perim,R,Uxs,Cd,tau);
param.Properties.VariableNames = {'x','Depth','BedElev','Area','Perimeter','R','Uxs','Cd','tau'};

% Plot data

if pflag == 1
plot(x,zchan,'r',x,zchan+ystand,'--g')
if grav<30
xlabel('x (m)')
ylabel('z and z_{water} (m)')
else
xlabel('x (ft)')
ylabel('z and z_{water} (ft)')
end
if flag==0
  title('Water Surface Profile using Euler Method')
elseif flag==1
  title('Water Surface Profile using Improved Euler Method')
elseif flag==2
  title('Water Surface Profile using Modified Euler Method')
elseif flag==3
  title('Water Surface Profile using Runge-Kutta (4th order) Method')
elseif flag==4
  title('Water Surface Profile using Standard Step Method')
```

```
end
  legend('Channel Bottom','Water Surface')
end
```

File: CMGeom.txt

```
Stationft,Stationm,ElevatonofbedmNAVD88,May2017mNAVD88,Apr2016mNAVD88,Elevationofwallm
NAVD88,wm,Bottomslopevbottomrunrise,Sidesloperunrise,manningsn
37214,11342.8272,3.48,NaN,3.48,7.3,9.73,10.35,0,0.022
34600,10546.08,0.09,0.15,0.09,4.12,9.73,10.35,0,0.022
34400,10485.12,-0.15,0.4,-0.12,3.89,10.01,10.66,0,0.03
33600,10241.28,-1.12,-0.08,-0.39,3.64,9.84,10.41,0,0.03
33160,10107.168,-1.65,-0.41,-0.66,3.94,10,7.99,0,0.03
32900,10027.92,-1.73,-0.72,-0.84,3.64,10.05,0,0,0.03
32700,9966.96,-1.83,-0.95,-0.95,3.64,9.93,0,0,0.03
32338,9856.6224,-1.85,-0.97,-1.19,3.65,10.01,0,0,0.03
31935,9733.788,-2.61,-0.8,-1.22,3.65,12.28,0,0,0.03
31900,9723.12,-2.62,NaN,-1.23,3.65,9.144,0,6,0.015
31890,9720.072,-1.97,NaN,-0.6,3.65,9.144,0,6,0.015
31850,9707.88,-1.98,NaN,-0.6,3.65,9.144,0,6,0.015
31700,9662.16,-2.13,NaN,-0.6,3.65,9.144,0,6,0.015
31000,9448.8,-2.28,NaN,-0.6,3.65,9.144,0,6,0.015
28204,8596.5792,-2.88,NaN,-0.6,3.65,24.384,0,6,0.015
28203,8596.2744,-2.88,NaN,-0.6,3.65,24.384,0,6,0.015
27000,8229.6,-2.88,NaN,-0.6,3.65,24.384,0,6,0.015
24400,7437.12,-2.88,NaN,-0.6,3.65,60,0,6,0.015
21800,6644.64,-2.88,NaN,-0.6,3.65,60,0,6,0.015
20000,6096,-2.88,NaN,-0.6,3.65,60,0,6,0.015
```

File: Tide.txt

```
MHHW,MHW,MTL,MLW,MLLW,NGVD29,NAVD88
1.76,1.58,0.95,0.32,-0.01,0.83,0
```

For more information concerning the research in this report, contact the
Director, California Water Science Center
U.S. Geological Survey
6000 J Street, Placer Hall
Sacramento, California 95819
https://ca.water.usgs.gov

Publishing support provided by the U.S. Geological Survey
Science Publishing Network, Sacramento Publishing Service Center

ISSN 2328-0328 (online)
https://doi.org/10.3133/sir20195070